Journal of Advanced Joining Processes 8 (2023) 100159

Contents lists available at ScienceDirect

Journal of Advanced Joining Processes

journal homepage: www.sciencedirect.com/journal/journal-of-advanced-joining-processes

Joining of hybrid busbars for E-Mobility: An economic and environmental study

João PM Pragana [a], Miguel ST Sapage [a], Rui FV Sampaio [a], Ivo MF Bragança [b], Ines Ribeiro [a], Carlos MA Silva [a], Paulo AF Martins [a,*]

[a] IDMEC, Instituto Superior Técnico, Universidade de Lisboa, Portugal
[b] CIMOSM, Instituto Superior de Engenharia de Lisboa, Instituto Politécnico de Lisboa, Portugal

ARTICLE INFO

Keywords:
Hybrid busbars
Joining by forming
Fastening
Welding
Process-based cost modelling
Life cycle assessment

ABSTRACT

This paper presents a model to evaluate and analyze the costs of joining hybrid (copper-aluminum) busbars when different production processes are deployed. The process-based cost model (PBCM) is built upon the subdivision of the production cycle in three different stages related with the fabrication or purchase of auxiliary joining elements, preparation of the individual copper and aluminum conductors, and final joining of the hybrid busbars. The total cost per hybrid busbar is obtained by converting the major physical, human, and financial resources associated with the production cycle into itemized costs that make use of the expenses in materials, labor working hours, number and usage time of machines and tools, among other production costs. Application of the PBCM is illustrated with three different joining processes and enriched with a life cycle assessment (LCA) focused on the environmental performance of hybrid busbars throughout its fabrication, service use and end of life. The combined economic and environmental sustainability analysis of joining hybrid busbars allows concluding that despite conventional fastening being the cheaper process it has the highest environmental impact due to the use of bolts, nuts and washers made from galvanized medium carbon steel. Injection lap riveting arises to be the most well-balanced process in terms of production cost and environmental impact.

Introduction

Current environmental priorities to reduce CO_2 emissions and fight climate change are prompting the replacement of internal combustion vehicles with electric vehicles due to its strong dependence on fossil fuels. The transportation sector is among the major contributors to greenhouse gas emissions (GHG) and is responsible for approximately 26 % of the total emissions of the European Union (EU). In 2019, cars accounted for nearly 44 % of these emissions (European Environmental Agency, 2022).

Recent uptake of electric cars is leading automakers to come up with innovative lightweight body-in-white designs built upon combination of carbon fiber reinforced polymer laminates with steel and aluminum sheets to compensate for the integration of heavy battery energy-storage systems. Busbars and busway trunking systems are also preferred to cabling systems for distributing electric power from batteries to the electric motor, electric power steering, and AC/DC converters, because they are easier to install and maintain (Das et al., 2019).

Busbars are commonly made from copper sheets or strips, hereafter referred to as 'the conductors', and their design is aimed at carrying the required amount of electric current under the conditions of use, without exceeding its temperature rating (i.e., without melting the conductor or its insulator, if existent). However, in the highly competitive transportation industry both the electro-thermo-mechanical performance of the busbars and the material and production costs need to be considered (Kirkpatrick, 1989).

In fact, the rising price of copper resulting from its key role in achieving the goal of an electrified, low carbon society, has been encouraging its total or partial replacement by lighter and cheaper conductive materials, such as aluminum. In the case of hybrid (copper-aluminum) busbars, this is accomplished by resizing the geometry and the cross-sections of the individual copper and aluminum conductors to ensure similar electrical conductance, while reducing the cost and weight up to 40 % (Kaufmann et al., 2023).

However, the utilization of hybrid busbars comes at the expense of raising difficulties in joining the copper and aluminum conductors due

* Corresponding author.
E-mail address: pmartins@tecnico.ulisboa.pt (P.A. Martins).

https://doi.org/10.1016/j.jajp.2023.100159

Available online 13 October 2023

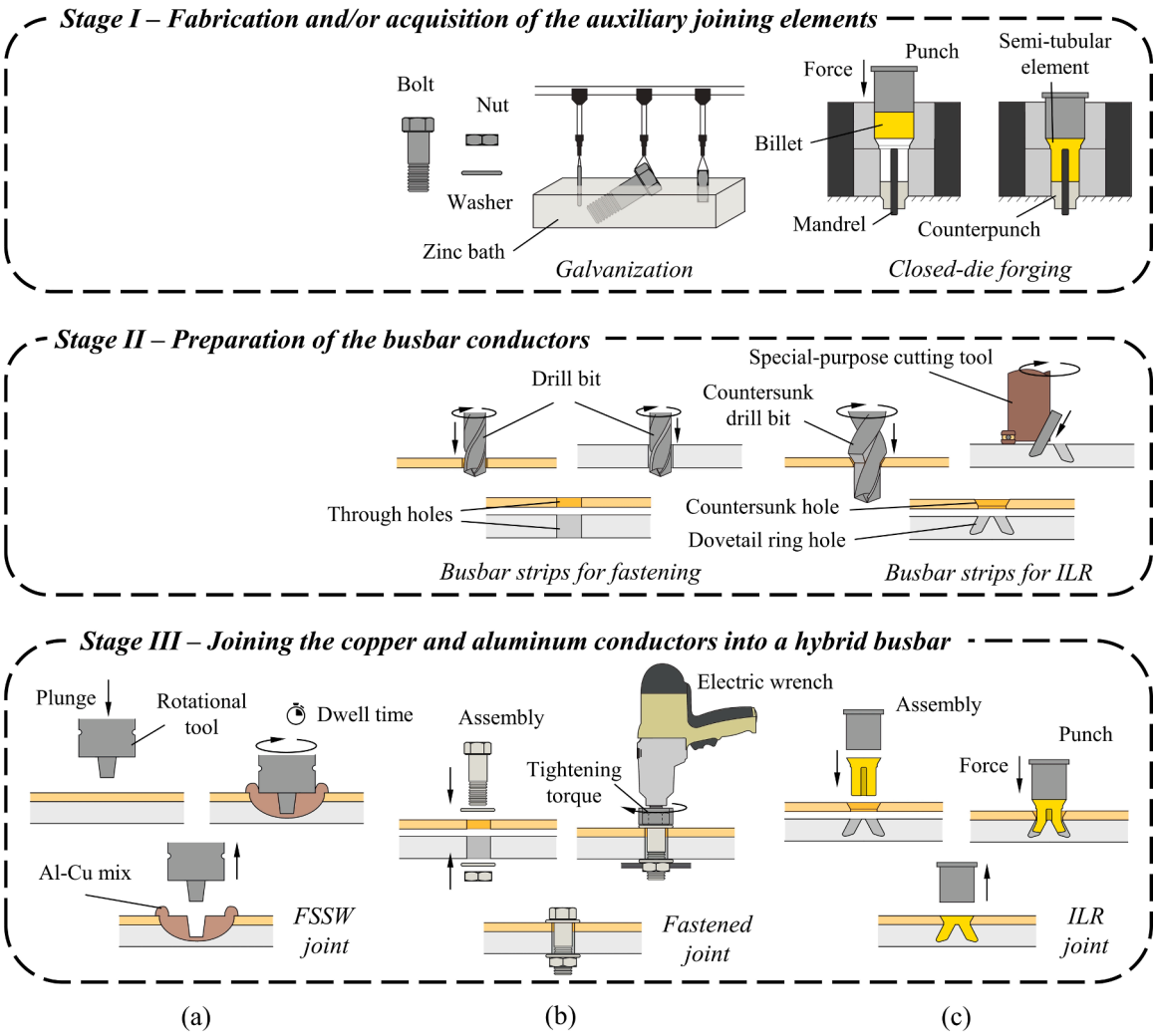

Fig. 1. Schematic representation of the production cycle for joining hybrid busbars in the case of (a) friction stir spot welding (FSSW), (b) conventional fastening (CF), and (c) injection lap riveting (ILR).

to differences in their cross-sections and in their physical and mechanical properties (Pragana et al., 2023). The available solutions for joining hybrid busbars are mainly based on the utilization of specific welding or mechanical joining processes.

In the case of welding, the preferred choices go to the use of friction stir welding, ultrasonic welding, and laser welding. Friction stir welding (FSW) and its variant friction stir spot welding (FSSW), in which there is no linear movement of the tool, are solid-state welding processes that can reduce the formation of brittle copper-aluminum intermetallic compounds that are commonly formed when the two materials are locally heated and metallurgically bonded together. FSW is suitable for the fabrication of copper-aluminum butt and lap hybrid busbar joints with good mechanical resistance and smooth surface quality, whereas FSSW is mainly used to produce spot welds having an exit hole of tool pin extraction. A more pronounced reduction of intermetallic components, which have poorer conductance than copper and aluminum, can be achieved if the tool pin offset is controlled with respect to the tool pin diameter and to the thickness of the joint (Yaduwanshi et al., 2018).

Ultrasonic welding (Silva et al., 2022) and electromagnetic pulse welding (Marya and Marya, 2004) are alternative solid-state welding processes that have been investigated and successfully utilized to produce lap joints in hybrid busbars. The joints can be completely free of intermetallic compounds and, therefore, capable of providing small disturbance of the current flow and good electrical performance (Bergmann et al., 2013). The absence of intermetallic compounds is a consequence of the joining mechanism of ultrasonic and electromagnetic pulse welding, which is mainly built upon interatomic and intermolecular forces at the contact interface between the two overlapped sheets (conductors). However, this is also the reason why both processes are limited to hybrid busbars made from very thin sheets and subjected to small loads.

Laser welding involves the use of high thermal energy density provided by a laser beam and allows producing lap and butt joints with very narrow heat affected zones due to selective and precise melting of the copper and aluminum sheets (conductors). However, the weld bead penetration is negatively affected by the highly reflective surfaces of copper and aluminum, namely in the case of lap joints. Intermetallic compounds are difficult to prevent but their amount can be kept at a minimum if the operating parameters are properly controlled. Examples of applications can be found in the connections of battery packs in electric cars (Sadeghian and Iqbal, 2022)

In the case of mechanical joining, the preferred choice goes to the fastening or joining by forming processes (Meschut et al., 2022). Both types of processes are carried out at room temperature and, therefore, avoid the formation of intermetallic compounds. However, fastening and joining by forming are not free of problems either.

Fastening, for example, gives rise to non-uniform local contact pressures that cause disturbance in the electric current flow due to the application of joining forces directly on the busbar conductor surfaces, by means of bolts and nuts. Consequently, the electric performance of

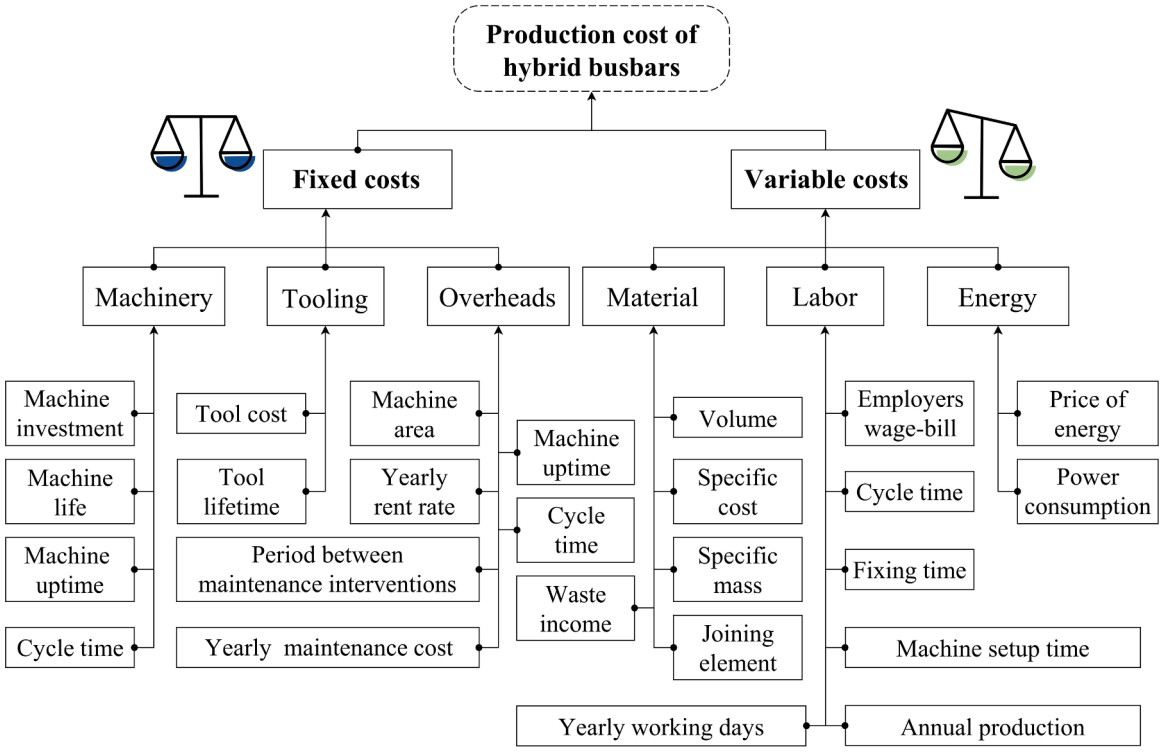

Fig. 2. Production cost chart of hybrid busbars.

fastened hybrid busbars is very sensitive to self-loosening in service and to disturbances of current flow caused by the higher electric resistivity of the bolts and nuts typically made from medium carbon steel (Sampaio et al., 2022). Still, fastened joints are easy to assemble and disassemble and are commonly used in busbars and busway trunking systems of electric cars (Rana et al., 2017).

The avoidance of self-loosening, the possibility of using permanent form-close and/or force closed joints subject to high contact pressures across wide overlapping areas, and the possibility of circumventing the use of auxiliary joining elements made from materials with higher electric resistivity than copper and aluminum has been driving attention towards the use of joining by forming processes. This type of mechanical joining processes includes those with auxiliary elements (e.g., self-pierce riveting, self-clinching and injection lap riveting) and those without auxiliary elements (e.g., clinching and sheet-bulk compression) (Meschut et al., 2022).

In recent years, the authors proposed and developed new joining by forming processes for the connection of monolithic and hybrid busbars (Sampaio et al., 2023). Some of these processes made use of auxiliary joining elements of copper or aluminum while others waived their use to minimize the disturbance of the electric current flow.

Although the electrical performance of hybrid busbars joints produced by some of these new joining by forming processes is generally better than that of similar joints fabricated by welding and conventional mechanical joining processes, in a competitive environment the decision to choose between the different processes requires consideration of the economic and environmental impact of the production cycle.

Optimization of process variables solely based on the electric performance of the hybrid busbars may be adequate to small-scale production, but process-based cost modeling (PBCM) is essential to support the choice of the joining process in medium and large-scale production. However, as recently shown by Varis (2006) and Nguyen et al. (2023) on their studies on clinching and friction stir welding, there is a considerable lack of information on the selection of processes and optimization of process variables according to economic-based criteria.

Under these circumstances, this paper aims to investigate the economic and environmental factors involved in the joining of hybrid busbars. For this purpose, the authors setup a PBCM to input and analyze the cost drivers of the three major stages of the production cycle for joining hybrid busbars: (i) the fabrication or purchase of auxiliary joining elements, (ii) the preparation of the busbar conductors, and (iii) the joining of hybrid busbars. The proposed PBCM is applied to a test case consisting of hybrid busbar joints fabricated by friction stir spot welding (FSSW), conventional fastening (CF), and injection lap riveting (ILR) with the objective of drawing the cost performance of each individual process. Life cycle assessment (LCA) to evaluate the environmental performance of each joining process is carried out to complement the economic-based criteria with sustainability insights.

Methods and procedures

Production cycle for joining hybrid busbars

Knowledge of the production cycle for joining hybrid busbars is essential to identify the major physical, human, and financial resources to include in the PBCM. Fig. 1 summarizes the production cycle for the three joining processes that were chosen by the authors: friction stir spot welding (FSSW), conventional fastening (CF) and injection lap riveting (ILR). FSSW and CF were chosen from the welding and mechanical joining group of processes that can be used to fabricate hybrid busbar joints. ILR is a new process belonging to the group of mechanical joining processes that was recently developed and applied by the authors in the fabrication of hybrid busbars.

As seen, the production cycle for joining hybrid busbars may be divided into three main stages:

a) Stage 1 - Fabrication and/or acquisition of the auxiliary joining elements that are used to connect the two different conductors,
b) Stage 2 - Preparation of the busbar conductors (sheets or strips) according to the ready-to-join requirements of each joining process,
c) Stage 3 - Joining the copper and aluminum conductors into a hybrid busbar.

According to Fig. 1 not all the processes encompass the three different stages of the production cycle. In the case of friction stir spot welding (FSSW), for example, there are no auxiliary joining elements, nor preparation of the conductors, which are joined in the as-supplied state. This justifies the reason why FSSW is only referred to Stage 3 (refer to Fig. 1). Likewise, the application of the PBCM to FSSW will not include the production or acquisition of auxiliary joining elements (Stage 1) nor the preparation of the busbar conductors for subsequent joining (Stage 2).

In contrast, both conventional fastening (CF) and injection lap riveting (ILR) make use of the auxiliary joining elements that are included in Stage 1 (Fig. 1). The bolts, nuts, and washers of CF can be easily purchased, but the semi-tubular rivets of ILR must be fabricated because they do not follow a standard and, therefore, are not available in the market.

Stage 2 also exists in CF and ILR processes because different types of holes need to be machined in order to prepare the copper and aluminum conductors for the joining operation of Stage 3. CF requires drilling through holes in both conductors, whereas ILR requires drilling dovetail ring and countersunk holes in the stronger and softer conductors, respectively.

Stage 3 in Fig. 1 allows understanding the differences between CF and ILR because the first only requires the application of a tightening torque on each bolt-nut pair to assemble the hybrid busbar, whereas the second requires injection of the semi-tubular rivet through the upper sheet into the dovetail ring hole of the lower sheet by compression with a punch.

Process-based cost modeling

The proposed PBCM was constructed with a threefold objective. Firstly, to establish a strong relation between the production cycle and the physical, human, and financial resources that contribute to the cost of a single hybrid busbar (also referred to as the 'per-part cost'). Secondly, to account for expected or unexpected changes in the production cycle. Thirdly, to allow calculating and comparing the cost of different processes to fabricate hybrid busbars before actual production.

The production cycle for joining hybrid busbars (Fig. 1) does not include additional stages related to the production of the raw materials (sheets and strips), design of the joints, shaping of the conductors into the required geometries, testing and inspection of the joints, and final packing and transportation because the associated costs are somewhat independent of the three joining processes under consideration. Under these circumstances, the model to evaluate the total cost C_{total} of joining hybrid busbars (hereafter referred to as 'the cost of hybrid busbars') when different processes are deployed is built upon two primary parcels: (i) the fixed costs C_{fix} and (ii) the variable costs C_{var}, whose details are summarized in Fig. 2 and explained in detail in the following subsections,

$$C_{total} = C_{fix} + C_{var} \tag{1}$$

Fixed costs

The fixed costs C_{fix} are the expenses that remain constant in the production cycle, regardless of the number of units fabricated. They include the machinery $C_{machinery}$ and tooling $C_{tooling}$ costs, considering depreciation, and the overheads $C_{overheads}$, also called indirect costs, which are indispensable for the overall production effort,

$$C_{fix} = C_{machinery} + C_{tooling} + C_{overheads} \tag{2}$$

The allocation of machinery costs $C_{machinery}$ is based on the machines that are utilized by each joining process - drilling and/or milling machines in the case of CF and ILR, presses in the case of ILR, and friction stir welding units in the case of FSSW. If all these machines are purchased on the premise that they will be used for other manufacturing purposes, the machinery costs $C_{machinery}$ per-part (i.e., per hybrid busbar) can be written as,

$$C_{machinery} = \sum_{i=1}^{n} \left(\frac{M_{machine}}{N_{life}} \times \frac{t_c}{t_u} \right)_i \tag{3}$$

The symbol n in the above equation refers to the total number of machines used in the whole production cycle. Then, for each machine i, $M_{machine}$ is the machine acquisition cost, N_{life} is the machine life span in years, t_c is the machine time for joining a hybrid busbar in a production cycle, and t_u is the machine uptime (i.e., the total available time of the machine in a production cycle). The ratio t_c/t_u corresponds to the utilization rate of each machine in view of non-dedicated equipment which are commonly implemented in functional layouts enabling flexible use for multiple tasks and workstations (Koren and Shpitalni, 2010 and Morgan et al., 2021).

The tooling costs $C_{tooling}$ encompass the purchase, deployment, and utilization of a broad category of tools such as, (i) metal cutters and holders for drilling and/or milling, (ii) rotational tools, fixtures and jigs for friction stir welding, and (iii) punch-die tool sets for forming and joining by forming operations. Thus, considering a production cycle that makes use of n different tools, the tooling costs $C_{tooling}$ per-part can be expressed as,

$$C_{tooling} = \sum_{i=1}^{n} \left(M_{tool} \times \frac{t_p}{t_l} \right)_i \tag{4}$$

where M_{tool} is the tool acquisition cost, t_p is the affiliated tool time directly associated with the production rate and t_l is the expected tool life.

The overhead costs $C_{overheads}$ comprise renting of the plant/laboratory and maintenance of the machines because insurance and other indirect costs, are not considered in the model. Their value per-part can be written as,

$$C_{overheads} = YRR \times \sum_{i=1}^{n} \left(MA \times \frac{t_c}{t_u} \right)_i + \sum_{i=1}^{n} \left(M_{maintenance} \times \frac{t_c}{t_u} \right)_i \tag{5}$$

The first term in the above equation refers to the renting costs, which are obtained from the yearly rent rate YRR of the plant/laboratory (per area) multiplied by the machine area MA and by the ratio t_c/t_u of the machine time t_c to the machine uptime t_u. The second term refers to the maintenance costs, which are calculated by multiplying the yearly expenses $M_{maintenance}$ by the ratio t_c/t_u.

Variable costs

The variable costs C_{var} are the expenses that are directly dependent on the production scale of hybrid busbars. They rise as production increases and fall as production decreases, and include the sum of the expenses that are affiliated with materials C_{mat}, labor C_{labor}, and energy consumption C_{energy},

$$C_{var} = (C_{mat} - I_{waste}) + C_{labor} + C_{energy} \tag{6}$$

The term $(C_{mat} - I_{waste})$ in the above equation refers to the net material cost, which is the cost of purchasing the materials C_{mat} subtracted from the income I_{waste} of reselling the scrap at the end of the production cycle. The breakdown of the net material cost per-part includes:

(i) the cost C_{fast} of purchasing the bolts, nuts, and washers, in the case of joining by CF,
(ii) the cost $\rho_{rivet} \times V_{rivet} \times C_{rivet}$ of fabricating the semi-tubular rivets, in the case of joining by ILR, where ρ_{rivet} is the specific mass, V_{rivet} is the volume, and C_{rivet} is the specific cost of the material used for producing rivets,
(iii) the income $\rho_{scrap} \times V_{scrap} \times C_{scrap}$ of the scrap produced in the production cycle, where ρ_{scrap} is the specific mass resulting from the different type of residues, V_{scrap} is the total scrap volume, and

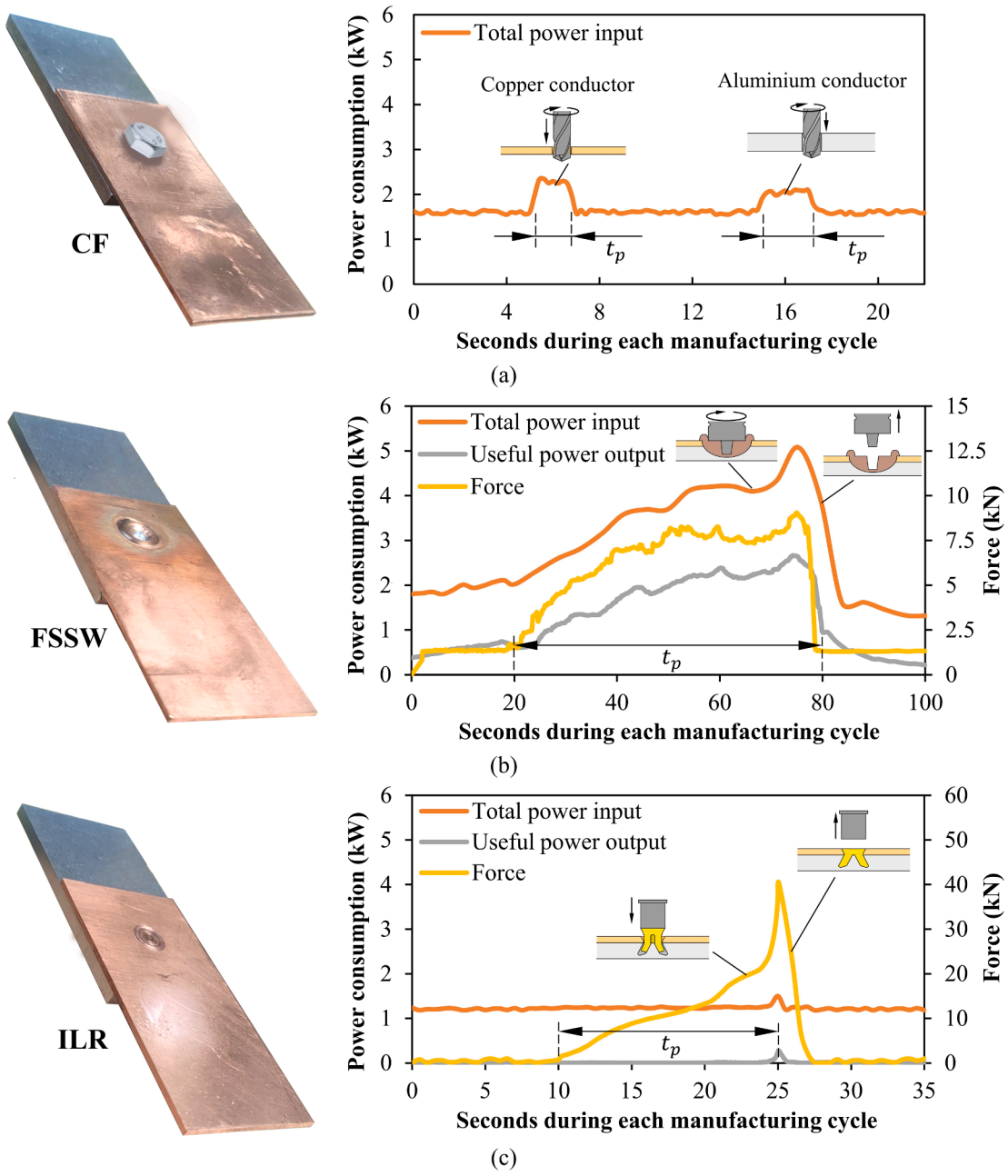

Fig. 3. Experimental measurements of the power consumptions and force during the manufacturing cycle time t_c (seconds) for the: (a) drilling stage of CF, (b) joining stage of FSSW and (c) joining stage of ILR. Photographs of the final hybrid busbar joints are included.

C_{scrap} is the waste income per mass. This term is negative because it reduces the net material cost.

$$(C_{mat} - I_{waste}) = C_{fast} + (\rho_{rivet} \times V_{rivet} \times C_{rivet}) - \sum_{i=1}^{n} (\rho_{scrap} \times V_{scrap} \times C_{scrap})_i \quad (7)$$

Labor costs C_{labor} are related to the payroll of the employes in tasks that are directly associated with the production cycle. In the proposed cost model, the labor costs are breakdown into three main parcels: (i) the affiliated machine time t_c, (ii) the fixing time t_{fixing}, and (iii) the machine setup time t_{setup}, per-part,

$$C_{labor} = M_{labor} \times \sum_{i=1}^{n} \left(t_c + t_{fixing} + \frac{t_{setup} \times WD}{AP} \right)_i \quad (8)$$

In the above equation, M_{labor} is the corresponds to wage-bill of the employes per unit of time, WD is the number of yearly working days and AP is the annual production of hybrid busbars. The inclusion of WD and AP in the third parcel allows converting the setup time t_{setup} from a daily basis to a time required per-part.

The energy costs C_{energy} are estimated from the power consumptions $P_{machine}$ during the machine time t_c per hybrid busbar, for all the machines, multiplied by the price of energy M_{energy}, as follows,

$$C_{energy} = M_{energy} \times \sum_{i=1}^{n} \int_0^{t_c} P_{machine} dt \quad (9)$$

Different power consumptions and machine times need to be considered because they depend on the type of machines utilized in the production cycle as well as on their corresponding active or idle states.

Life cycle assessment

Sustainability insights on the three different joining processes to fabricate hybrid busbars were evaluated through life cycle assessment (LCA). This methodology allows measuring, analyzing, and comparing the environmental performance of each process by adopting a cradle-to-gate scope based on raw material extraction and subsequent manufacturing tasks.

Data to be used in LCA comprises direct resources such as energy and materials required by the joining processes, and indirect resources and emissions taken from the Ecoinvent 3.8 (Ecoinvent, 2022) global averages database. The environmental performance is quantified by means of different impact category indicators using the ReCiPe2016 methods at midpoint and endpoint levels (Huijbregts et al., 2017) available in the SimaPro 7 software.

Firstly, the ReCiPe method at midpoint level (Midpoint (H) V1.11/World ReCiPe H) is used for transforming data (life cycle inventory) into midpoint indicators among the chosen impact categories. In this method, the impact in each category is translated into a particular unit. Eventually, the ReCiPe method at endpoint level (Endpoint (H) V1.11/World ReCiPe H/H) is used for transforming the different midpoint impact category indicators into three main categories: human health, ecosystems, and resources, due to its easier assessment in terms of environmental relevance. This methodology brings some subjectivity into the analysis due to normalization and weighting, but it is useful to compare different technological alternatives due to the utilization of a single unit. However, the subjectivity can be mitigated when combined with the previous midpoint analysis (Kokare et al., 2023)

Test case

Verification of the proposed PBCM and LCA methodologies is a necessary step before a process being accepted and adopted for widespread use. For this purpose, AA6082-T6 aluminum and C11000 copper strips (conductors) with 100 mm length and 50 mm width were cut out from sheets with 5 mm and 2 mm thickness. The utilization of aluminum and copper strips with a cross-section ratio of 2.5 is necessary to ensure near identical conductance in both strips, due to the higher electric resistivity of aluminum (Sampaio et al., 2022a).

The joining of the hybrid busbars was carried out with three different processes: FSSW, CF and ILR. In the case of FSSW, the joints were fabricated in an ESAB Legio FSW3U machine using a rotational tool with a shoulder diameter of 16 mm and a taper cylindrical pin with a diameter of 5 mm. In the case of CF, the copper and aluminum conductors were clamped together with a tightening torque of 20 Nm applied by an electric wrench on a M8 hexagonal head bolt-nut pair made from galvanized medium carbon steel (class 8.8) and two washers. In the case of ILR, the joints were produced at room temperature in a punch-die tool set installed in a Instron SATEC 1200 kN hydraulic testing machine.

The metal cutting operations for cutting the through holes required by CF, and the countersunk and dovetail ring holes required by ILR were carried out in the Haas Mini Mill 2. Drill bits coupled in collet chuck holders were used for drilling through and countersunk holes whereas the dovetail ring holes were cut using a special purpose tool with HSS cutters that was recently developed by the authors (Ferreira et al., 2021). Information regarding the operating parameters for each cutting operation can be found in the previous reference.

The main cost assets of the production cycle were listed, and the duration of each task was determined onsite. The power consumption of the machines was measured with a power meter PROVA 6830 equipped with clamp-on ammeters and voltage test leads. The consumptions were recorded in 0.2 s time intervals with a resolution 1 W for power supplies up to 10 kW during the complete range of the cycle time t_c for each manufacturing stage.

Fig. 3 discloses the power consumption (designated as 'total power input') and of the power output that was effectively used to carry out each manufacturing process ('useful power output') per-part. Force evolutions are included to give a perspective of what is occurring during the cycle time.

The input data for the proposed PBCM and LCA was retrieved from experiments with the three different joining processes and is summarized in Table 1.

Table 1
Input data for the PBCM and LCA. Refer to Fig. 1 for process details.

Common input data			
Annual production	1000,000 parts/year	**Direct Wages**	10 €/hour
Yearly rent rate	1000 €/year	**Price of Energy**	0.15 €/kWh
Machine uptime	1920 h/year	**Worker dedication**	100%
Machine life	5 years	**Material cost (copper)**	11.69 €/kg
Yearly working days	240 days/year	**Copper waste income**	0.74 €/kg
Yearly maintenance cost	1000 €/year	**Aluminum waste income**	0.37 €/kg
Conventional fastening (CF)			
Tool Cost	1500 €	**Production time**	3 s/part
Tool lifetime	20 min	**Machinery area**	9 m^2
Machine investment	70,000 € (drilling) and 500 € (joining)		
Cycle time	22 s (drilling) and 20 s (joining)		
Machine nominal power	5.6 kW (drilling) and 0.5 kW (joining)		
Machine setup time	30 min/day (drilling) and 5 min/day (joining)		
Energy consumption	35.24 kJ/part (drilling) and 5.05/part (joining)		
Material consumption	3.13 g/part (washers), 7.4 g/part (nut) and 15.82 g/part (bolt)		
Material waste	0.91 g/part (copper) and 0.68 g/part (aluminum)		
Friction stir spot welding (FSSW)			
Tool cost	700 €	**Machine setup time**	15 min/day
Tool lifetime	1500 min	**Production time**	60 s/part
Machine investment	150,000 €	**Machinery area**	6 m^2
Cycle time	100 s/part	**Fixing time**	5 min/part
Machine nominal power	30 kW	**Fixture cost**	5000 €
Energy consumption	353.6 kJ/part (joining)		
Material consumption	–	**Material waste**	–
Injection lap riveting (ILR)			
Cutting tool cost	750 € (drilling), 2000 € (special purpose tool) and 20 € (metal cutters)		
Cutting tool life	20 min (drilling), 50,000 parts (special purpose tool) and 2 min (metal cutters)		
Cutting time	1.5 s (drilling) and 5 s (metal cutters)		
Forming tool cost	10,000 € (rivet forging) and 2000 € (joining)		
Forming tool life	25,000 parts (rivet forging) and 50,000 parts (joining)		
Machine investment	70,000 € (cutting), 100,000 € (rivet forging), and 100,000 € (joining)		
Machine setup time	30 min/day (cutting), 20 min/day (rivet forging) and 20 min/day (joining)		
Machine nominal power	5.6 kW (cutting), 20 kW (rivet forging) and 20 kW (joining)		
Cycle time	25 s (cutting), 20 s (rivet forging) and 35 s (joining)		
Machinery area	9 m^2(cutting), 2 m^2 (rivet forging) and 2 m^2 (joining process)		
Energy consumption	17.19 kJ/part (rivet forging), 40.05 kJ/part (drilling), and 30.08 kJ/part (joining)		
Material consumption	3.47 g/part (copper)		
Material waste	1.41 g/part (copper) and 0.58 g/part (aluminum)		

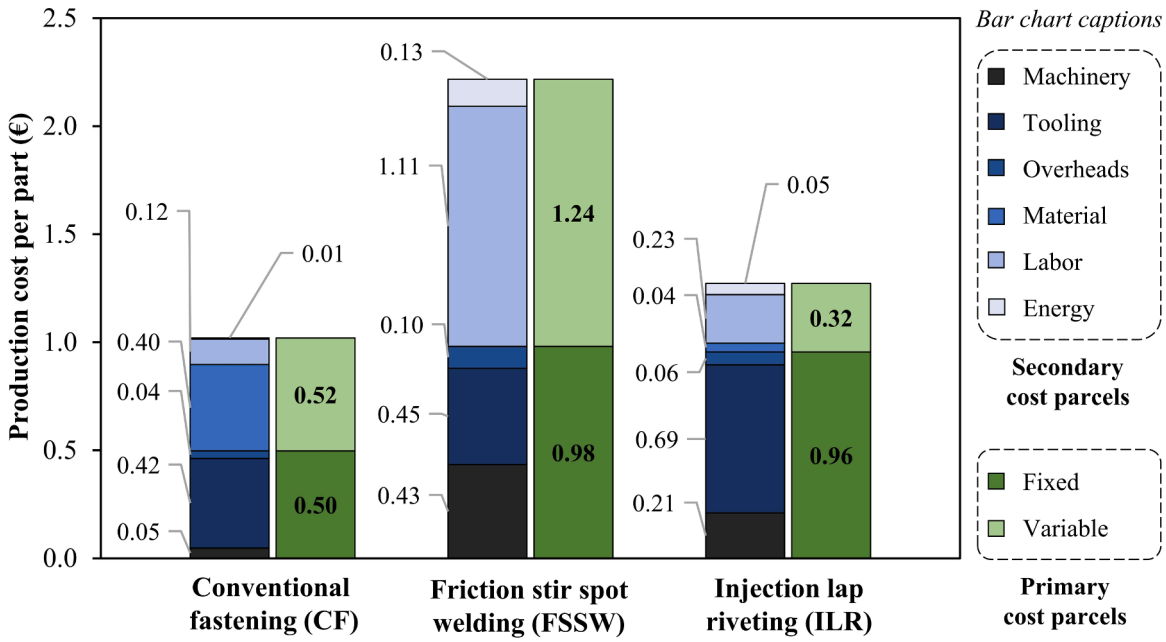

Fig. 4. Breakdown of total costs for the three different joining processes on a per-part (i.e., per hybrid busbar) basis.

Results and discussion

Cost drivers

Cost performance of the three different processes for joining hybrid busbars was assessed using the proposed PBCM with the input data provided in Table 1. Fig. 4 shows the breakdown of total costs into fixed and variable costs and into their main individual cost drivers, to allow cost analysis to be done on a per-part scale (i.e., per hybrid busbar), rather than on a total annual basis.

As seen, conventional fastening (CF) stands out as the cheapest joining process with a production cost of 1.02 € per part whereas friction stir spot welding (FSSW) sticks out as the most expensive with a cost per-part over two times greater (2.22 € per-part). Results also show that variable costs play a slightly superior role in FSSW (about 56 %) and a much inferior role in injection lap riveting (ILR) (only 25 %) while in the case of CF both primary cost parcels are nearly even (refer to the green bars in Fig. 4).

The differences in the relative importance of fixed and variable costs reflect the various aspects of cost production for the three joining processes (refer to the blue bars of the secondary cost parcels in Fig. 4). In the case of CF, material costs have the largest contribution to total cost due to the necessity of purchasing several auxiliary joining elements (bolt, nut, and washers). In connection to this, it is worth remembering that the costs of the copper and aluminum strips (conductors) are not included in the model because they are identical for the three joining processes.

FSSW leads to a different conclusion because no auxiliary joining

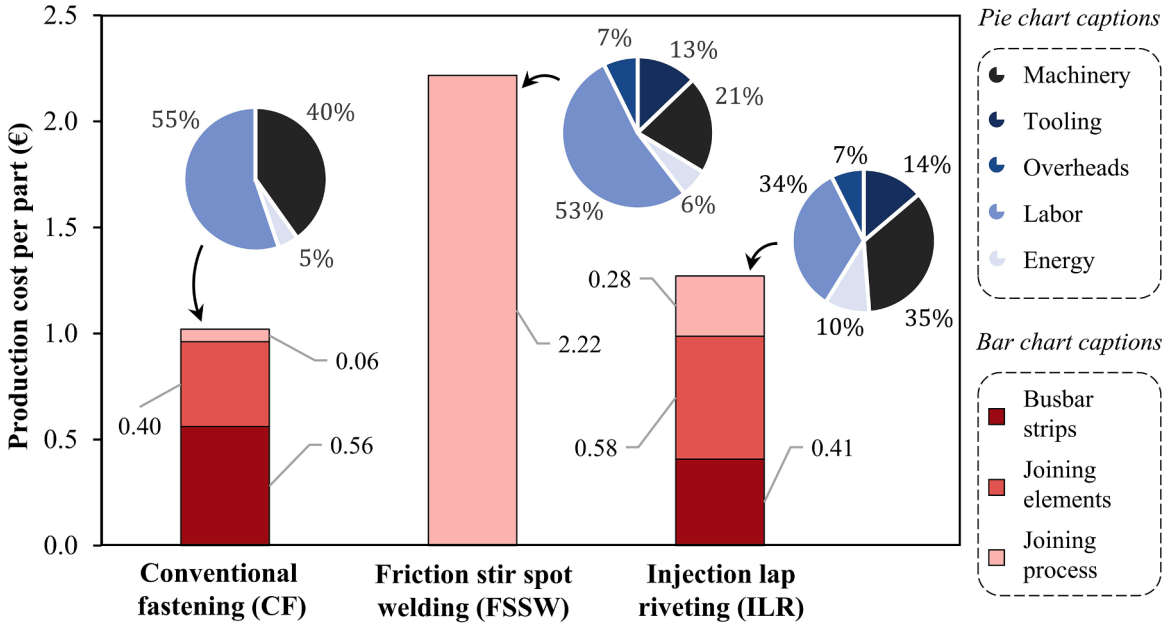

Fig. 5. Cost activities of CF, FSSW and ILR for producing hybrid busbars. The blue pie charts refer to the individual cost parcels applicable to the manufacturing tasks of each joining process.

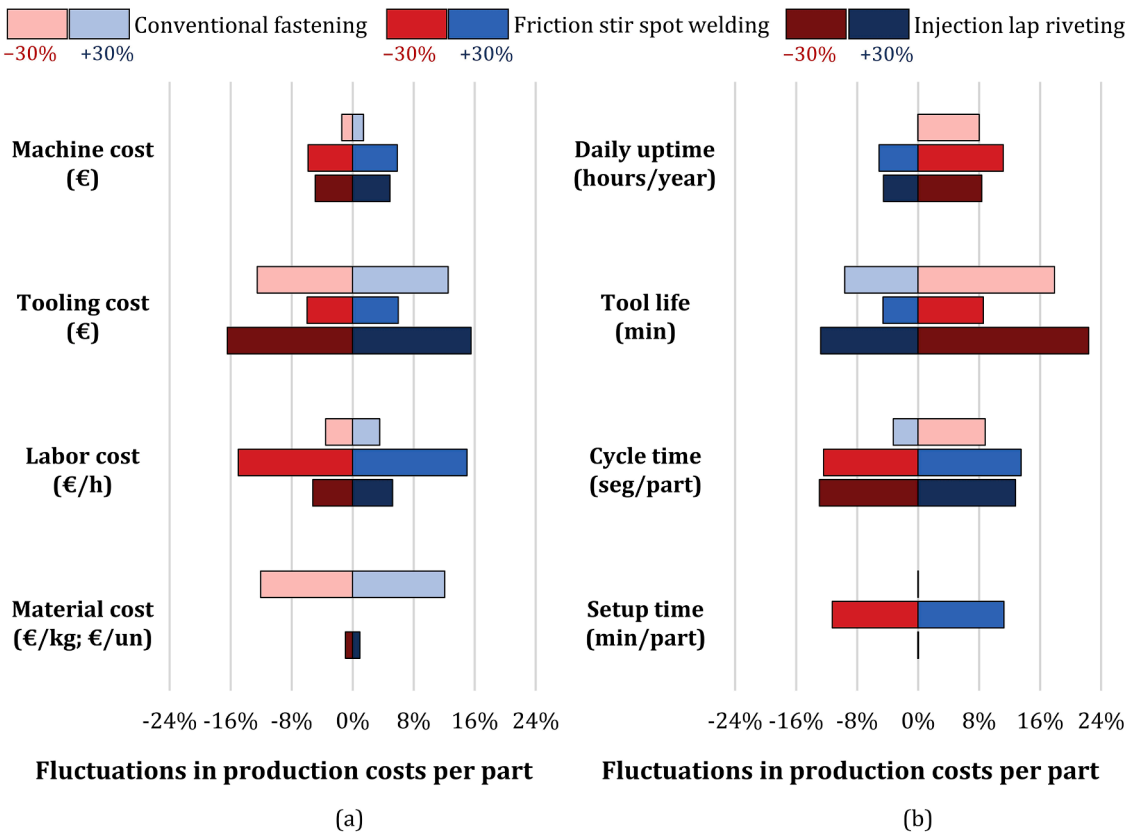

Fig. 6. Sensitivity analysis of the PBCM built upon ± 30% variation of the (a) capital-based and (b) time-based variables.

elements are used. In fact, the largest contribution to total costs comes from the labor costs due to the high production cycle times of welding, and to the time spent in fixing and setting up the individual conductors for subsequent joining.

In the case of ILR, the larger contributions to total costs come from the fixed costs arising from tooling expenses at the different stages of the production cycle. These include the cutting tools used to fabricate the countersunk and dovetail ring holes as well as the punch-die tool sets used for fabricating the semi-tubular rivets and to join the individual copper and aluminum conductors into hybrid busbars. Because fixed costs can be spread over an increasing production scale, it may be concluded that the competitivity of injection lap riveting is expected to rise rapidly with expansion of the quantity of hybrid busbars produced.

Fig. 5 presents a different perspective by breaking the costs down into the tasks that are directly related to manufacturing. In CF, for example, the cost per-part is somewhat leveled by the preparation of the busbar strips (conductors) due to the involved cutting equipment. This is not the case in ILR, where the activities related to the production of the auxiliary joining elements assume the largest share (approximately 50 %) due to the higher acquisition cost and lower life expectancy of the forging tools used to fabricate the semi-tubular rivets, in contrast to the open die forging tools used in joining by forming. The result obtained for FSSW is once again influenced by both its high production cycle times and fixing times.

The blue pie charts included in Fig. 5 allow understanding the contributions of each individual cost parcel in the manufacturing tasks focused on each joining process. CF is dominated by the labor-intensive use of an electric wrench for tightening the final busbar joints. Labor costs are also predominant in FSSW due to its high production cycle times. Another important percentage of costs in FSSW is related to machine investments and tool wear, which limits the lifespan.

ILR presents a more even distribution of the individual cost parcels with special emphasis placed on labor and machinery costs that are likely caused by the fact that the test case experiments were carried out in a testing machine instead of a dedicated industrial press.

Cost sensitivity analysis

This section recalculates the production cost per-part for two alternative scenarios built upon quantitative variations of selected parameters of the input data of Table 1, to compare the new estimates with the original ones. In the first scenario (named as the 'capital scenario'), all capital-based variables are allowed to change within extreme values of ± 30 %. In the second scenario (named as 'time scenario'), all time-based variables are allowed to change within a similar range. Results for the capital and time scenarios are disclosed in Fig. 6a and b, respectively.

As illustrated in the figure, the first scenario built upon changes in the capital-based variables is highly dependent on the process for joining hybrid busbars. CF, for example, reveals significant dependence on tooling and material costs due to the limited lifespan of drilling bits and to the need of buying the auxiliary joining elements. FSSW presents an opposite cost dynamic with smaller sensitivity to tooling costs, no-sensitivity to material costs (because the process makes no use of auxiliary joining elements), and bigger sensitivity to labor costs due to the high cycle times of welding. Still, variations in tooling cost and in machinery costs can have a significant influence on the total cost per part.

Results for ILR allow understanding that total costs are strongly influenced by variations in tooling costs due to the wide variety of tools used in the whole production cycle. Still, the consequence of this dependence on total costs is somewhat diluted by the small sensitivity of the remaining capital-based costs.

In contrast to the capital-based scenario (Fig. 6a), which gives rise to a symmetric cost-sensitivity output, the changing prices of time-based variables generally lead to unsymmetric responses on the total cost

Table 2
– LCA midpoint level results.

Impact category (UNIT)	FSSW	CF	ILR
Global warming (kg CO_2 eq.)	8.06E-02	6.41E-02	2.30E-02
Stratospheric ozone depletion (kg CFC-11 eq.)	1.35E-08	1.65E-08	4.19E-09
Ionizing radiation (kBq Co-60 eq.)	3.33E-04	1.82E-03	2.03E-04
Ozone formation, Human health (kg NOx eq.)	2.18E-04	1.57E-04	6.30E-05
Fine particulate matter formation (kg PM2.5 eq.)	1.47E-04	1.16E-04	3.99E-05
Ozone formation, Terrestrial ecosystems (kg NOx eq.)	2.18E-04	1.64E-04	6.32E-05
Terrestrial acidification (kg SO_2 eq.)	4.73E-04	2.15E-04	1.28E-04
Freshwater eutrophication (kg P eq.)	7.96E-09	3.01E-05	4.83E-09
Marine eutrophication (kg N eq.)	1.11E-07	2.72E-06	4.57E-08
Terrestrial ecotoxicity (kg 1.4-DCB)	4.49E-02	3.47E-01	1.14E-02
Freshwater ecotoxicity (kg 1.4-DCB)	3.14E-06	5.07E-03	1.17E-06
Marine ecotoxicity (kg 1.4-DCB)	4.53E-05	7.03E-03	1.17E-05
Human carcinogenic toxicity (kg 1.4-DCB)	3.46E-05	7.61E-02	1.01E-05
Human non-carcinogenic toxicity (kg 1.4-DCB)	1.68E-03	6.33E-02	4.66E-04
Land use (m^2a crop eq.)	0.00E+00	1.18E-03	0.00E+00
Mineral resource scarcity (kg Cu eq.)	1.43E-06	2.67E-03	1.12E-04
Fossil resource scarcity (kg oil eq.)	1.81E-02	1.33E-02	5.20E-03
Water consumption (m^3)	1.11E-04	5.19E-04	1.33E-04

per-part (Fig. 6b). Machine uptime and tool life, for example, experience a stronger negative influence on total cost (i.e., an increase on total cost per-part) than other time-based variables, when their values rise. The changes in setup time are only significant to FSSW (Fig. 6b) and justify its strong dependence on the changes in labor costs (Fig. 6a).

To conclude it is worth mentioning that the unsymmetric cost-sensitivity output of the cycle time of CF, allows understanding that lowering the production rate does not necessary lead to a proportional reduction in total cost, as in the case of FSSW and ILR due to the number and type of machines involved in the whole production cycle.

Life cycle assessment

Following a similar approach to that used in the PBCM, the aluminum and copper sheet materials were not considered in LCA, as they are independent of the joining processes. The direct emissions of FSSW were also not considered because they are negligible (Shrivastava et al., 2015).

Table 2 shows the LCA midpoint level results calculated from the energy and material consumption and waste of Table 1, for each joining process. Results show that FSSW performs worst in the global warming category indicator due to its greater energy consumption (8.06E-02 kg CO_2 eq.) and CF presents the highest impact for the mineral resource scarcity given the amount of medium carbon steel required for the auxiliary joining elements (2.67E-03 kg Cu eq.).

Utilization of the ReCiPe method at endpoint level was subsequently done to combine the different midpoint impact category indicators of Table 2 into three main categories (human health, ecosystems, and resources) for each joining process. The results are shown in Fig. 7 and allow concluding that CF is the most eco-unfriendly process due to its high impact in human health (6.3 mPts) caused by the utilization of auxiliary joining elements made from medium carbon steel. The environmental impact of FSSW is 57 % smaller than that of CF but still 72 % greater than that of ILR, which is the most eco-friendly process, due to its lower impact on human health, ecosystems, and resources.

Conclusions

A new process-based cost model (PBCM) built upon the subdivision of the production cycle in three different stages related with the fabrication (or purchase) of auxiliary joining elements, preparation of the individual copper and aluminum conductors, and final joining of the hybrid busbars allows concluding that conventional fastening (CF) is the cheapest process. In contrast, friction stir spot welding (FSSW) is the most expensive with a production cost per-part over two times greater than that of CF.

The unsymmetric cost-sensitivity output of the cycle time of CF, allows understanding that lowering the production rate does not necessary lead to a proportional reduction in total cost, as in the case of FSSW and injection lap riveting (ILR) due to the number and type of machines involved in the whole production cycle.

In the case of ILR, despite its the total costs being strongly influenced

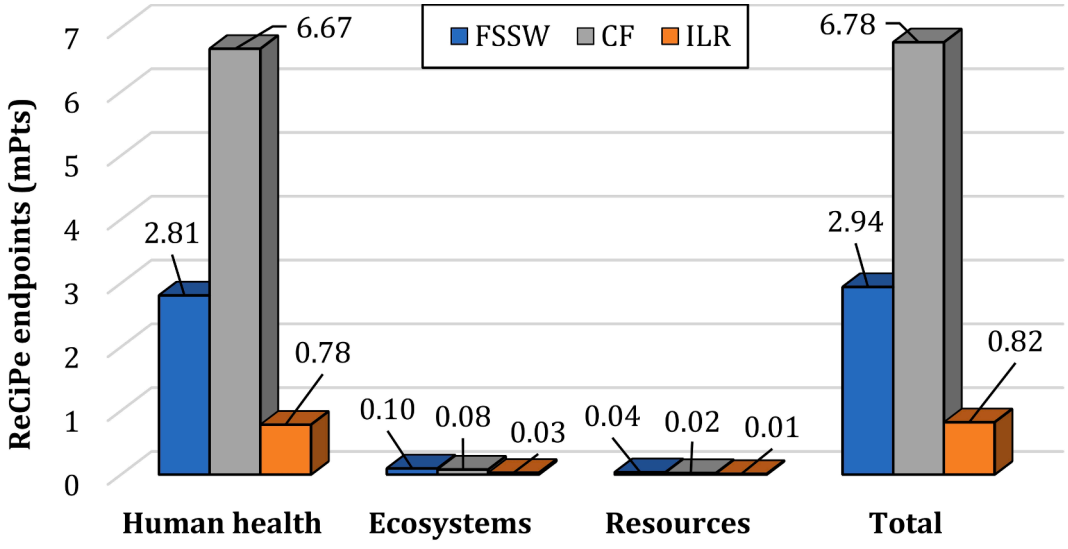

Fig. 7. LCA endpoint level results.

by variations in tooling costs due to the wide variety of tools used in the entire production cycle, the dependence is somewhat diluted by the small sensitivity of the remaining capital-based costs.

Life cycle assessment (LCA) shows that CF is the most eco-unfriendly process due to its high impact on human health caused by the utilization of auxiliary joining elements made from medium carbon steel. The environmental impact of FSSW is 57 % smaller than that of CF but still 72 % greater than that of ILR, which is the most eco-friendly process, due to its lower impact on human health, ecosystems, and resources.

Combining the economic and environmental sustainability impact at once, one can conclude that ILR is the best of the three processes that were selected to illustrate the application of these methodologies to the joining of hybrid busbars.

Declaration of Competing Interest

The authors declare that they have no known competing financial interests or personal relationships that could have appeared to influence the work reported in this paper.

Data availability

Data will be made available on request.

Acknowledgments

The authors would like to thank the support of Fundação para a Ciência e a Tecnologia of Portugal (FCT) and IDMEC, under LAETA - UIDB/50022/2020 and PTDC/EME-EME/0949/2020. Rui Sampaio would also like to acknowledge the support under the PhD Studentship 2022.12351.BD.

References

Bergmann, J.P., Petzoldt, F., Schürer, R., Schneider, S., 2013. Solid-state welding of aluminum to copper - Case studies. Weld. World 57, 541–550. https://doi.org/10.1007/s40194-013-0049-z.

Das, A., Barai, A., Masters, I., Williams, D., 2019. Comparison of tab-to-busbar ultrasonic joints for electric vehicle Li-ion battery applications. World Electr. Veh. J. 10, 55. https://doi.org/10.3390/wevj10030055.

Ecoinvent, 2022. Ecoinvent v3.8. Available at. https://ecoinvent.org/the-ecoinvent-database/data-releases/ecoinvent-3-8/ (Acessed August 1, 2023).

European Environment Agency, 2022. Transport and Environment Report 2022 - Digitalisation in the Mobility System: Challenges and Opportunities. https://doi.org/10.2800/47438. Luxembourg.

Ferreira, F.R., Pragana, J.P.M., Bragança, I.M.F., Silva, C.M.A., Martins, P.A.F., 2021. Injection lap riveting. CIRP Ann. – Manuf. Technol. 70, 261–264. https://doi.org/10.1016/j.cirp.2021.03.018.

Huijbregts, M.A., Steinmann, Z.J., Elshout, P.M., Stam, G., Verones, F., Vieira, M., Zijp, M., Hollander, A., Van Zelm, R., 2017. ReCiPe2016: a harmonised life cycle impact assessment method at midpoint and endpoint level. Int. J. Life Cycle Assess. 22, 138–147. https://doi.org/10.1007/s11367-016-1246-y.

Kaufmann, F., Strugulea, M., Höltgen, C., Roth, S., Schmidt, M., 2023. Seam oroperties of overlap welding strategies from copper to aluminum using green laser radiation for battery tab connections in electric vehicles. Materials (Basel) 16, 1069. https://doi.org/10.3390/ma16031069.

Kirkpatrick, L., 1989. Aluminum Electrical Conductor Handbook, 3rd Edition. The Aluminum Association, Arlington, USA.

Kokare, S., Oliveira, J.P., Godina, R., 2023. A LCA and LCC analysis of pure subtractive manufacturing, wire arc additive manufacturing, and selective laser melting approaches. J. Manuf. Process. 101, 67–85. https://doi.org/10.1016/j.jmapro.2023.05.102.

Koren, Y., Shpitalni, M., 2010. Design of reconfigurable manufacturing systems. J. Manuf. Syst. 29, 130–141. https://doi.org/10.1016/j.jmsy.2011.01.001.

Marya, M., Marya, S., 2004. Interfacial microstructures and temperatures in aluminium–copper electromagnetic pulse welds. Sci. Technol. Weld. Joining 9, 541–547. https://doi.org/10.1179/174329304X8685.

Meschut, G., Merklein, M., Brosius, A., Drummer, D., Fratini, L., Füssel, U., Gude, M., Homberg, W., Martins, P.A.F., Bobbert, M., Lechner, M., Kupferf, R., Groger, B., Han, D., Kalich, J., Kappe, F., Kleffel, T., Kohler, D., Kuball, C.M., Popp, J., Romisch, D., Troschitz, J., Wischer, C., Wituschek, S., Wolf, M., 2022. Review on mechanical joining by plastic deformation. J. Adv. Join. Process. 5, 100113 https://doi.org/10.1016/j.jajp.2022.100113.

Morgan, J., Halton, M., Qiao, Y., Breslin, J.G., 2021. Industry 4.0 smart reconfigurable manufacturing machines. J. Manuf. Syst. 59, 481–506. https://doi.org/10.1016/j.jmsy.2021.03.001.

Nguyen, T.T., Nguyen, C.T., Van, A.L., 2023. Sustainability-based optimization of dissimilar friction stir welding parameters in terms of energy saving, product quality, and cost-effectiveness. Neural. Comput. Appl. 35, 5221–5249. https://doi.org/10.1007/s00521-022-07898-8.

Pragana, J.P.M., Sampaio, R.F.V., Bragança, I.M.F., Silva, C.M.A., Martins, P.A.F., 2023. A joining by plastic deformation process to fabricate butt joints in copper-aluminium busbars. CIRP J. Manuf. Sci. Technol. 43, 205–213. https://doi.org/10.1016/j.cirpj.2023.04.008.

Rana, B., Mallick, P., Rana, T.K., Basu, D., Biswas, A.N., Pramanik, S., 2017. Efficient and superior elbow joint for high power busway trunking system. In: Proceedings of the 8th Annual Industrial Automation and Electromechanical Engineering Conference (IEMECON). Bangkok, Thailand.

Sadeghian, A., Iqbal, N., 2022. A review on dissimilar laser welding of steel-copper, steel-aluminum, aluminum-copper, and steel-nickel for electric vehicle battery manufacturing. Opt. Laser Technol. 146, 107595 https://doi.org/10.1016/j.optlastec.2021.107595.

Sampaio, R.F.V., Pragana, J.P.M., Bragança, I.M.F., Silva, C.M.A., Nielsen, C.V., Martins, P.A.F., 2022. Electric performance of fastened hybrid busbars: an experimental and numerical study. J. Mater. 236, 1152–1163. https://doi.org/10.1177/14644207211043009.

Sampaio, R.F.V., Pragana, J.P.M., Bragança, I.M.F., Silva, C.M.A., Martins, P.A.F., 2023. Thermo-electrical performance of hybrid busbars: an experimental and numerical investigation. J. Mater. 237, 70–80. https://doi.org/10.1177/14644207221102514.

Sampaio, R.F.V., Zwicker, M.F.R., Pragana, J.P.M., Bragança, I.M.F., Silva, C.M.A., Nielsen, C.V., Martins, P.A.F., 2022a. Busbars for E-mobility: state-of-the-art review and a new joining by forming technology. In: Davim, J.P. (Ed.), Mechanical and Industrial Engineering. Materials Forming, Machining and Tribology. Springer, Cham, pp. 111–141. https://doi.org/10.1007/978-3-030-90487-6_4.

Shrivastava, A., Krones, M., Pfefferkorn, F.E., 2015. Comparison of energy consumption and environmental impact of friction stir welding and gas metal arc welding for aluminum. CIRP J. Manuf. Sci. Technol. 9, 159–168. https://doi.org/10.1016/j.cirpj.2014.10.001.

Silva, R.G.N., De Meester, S., Faes, K., De Waele, W., 2022. Development and evaluation of the ultrasonic welding process for copper-aluminium dissimilar welding. J. Manuf. Mater. Process. 6, 6. https://doi.org/10.3390/jmmp6010006.

Varis, J., 2006. Economics of clinched joint compared to riveted joint and example of applying calculations to a volume product. J. Mater. Process. Technol. 172, 130–138. https://doi.org/10.1016/j.jmatprotec.2005.09.009.

Yaduwanshi, D.K., Bag, S., Pal, S., 2018. On the effect of tool offset in hybrid-FSW of copper-aluminium alloy. Mater. Manuf. Processes 33, 277–287. https://doi.org/10.1080/10426914.2017.1279309.